Geophysical Research Letters

RESEARCH LETTER

10.1029/2020GL092162

Tropical Stratospheric Circulation and Ozone Coupled to Pacific Multi-Decadal Variability

Fernando Iglesias-Suarez[1,2], Oliver Wild[2], Douglas E. Kinnison[3], Rolando R. Garcia[3], Daniel R. Marsh[4,5], Jean-François Lamarque[4], Edmund M. Ryan[6], Sean M. Davis[7], Roland Eichinger[1,8], Alfonso Saiz-Lopez[9], and Paul J. Young[2,10]

[1]Deutsches Zentrum für Luft- und Raumfahrt (DLR), Institut für Physik der Atmosphäre, Oberpfaffenhofen, Germany, [2]Lancaster Environment Centre, Lancaster University, Lancaster, UK, [3]Atmospheric Chemistry Observations and Modelling, NCAR, Boulder, CO, USA, [4]Climate and Global Dynamics Laboratory, NCAR, Boulder, CO, USA, [5]Faculty of Engineering and Physical Sciences, University of Leeds, Leeds, UK, [6]Department of Mathematics, University of Manchester, Manchester, UK, [7]NOAA Chemical Sciences Laboratory, Boulder, CO, USA, [8]Department of Atmospheric Physics, Faculty of Mathematics and Physics, Charles University, Prague, Czech Republic, [9]Department of Atmospheric Chemistry and Climate, Institute of Physical Chemistry Rocasolano, CSIC, Madrid, Spain, [10]Centre of Excellence for Environmental Data Science, a partnership between Lancaster University and the UK Centre for Ecology and Hydrology, Lancaster, UK

Abstract Observational and modeling evidence suggest a recent acceleration of the stratospheric Brewer-Dobson circulation (BDC), driven by climate change and stratospheric ozone depletion. However, slowly varying natural variability can compromise our ability to detect such forced changes over the relatively short observational record. Using observations and chemistry-climate model simulations, we demonstrate a link between multi-decadal variability in the strength of the BDC and the Interdecadal Pacific Oscillation (IPO), with knock-on impacts for composition in the stratosphere. After accounting for the IPO-like variability in the BDC, the modeled trend is approximately 7%–10% dec^{-1} over 1979–2010. Furthermore, we find that sea surface temperatures explain up to 50% of the simulated decadal variability in tropical mid-stratospheric ozone. Our findings demonstrate strong links between low-frequency variability in the oceans, troposphere and stratosphere, as well as their potential importance in detecting structural changes in the BDC and future ozone recovery.

Plain Language Summary Natural variability is a key element of the climate system and can mask human-induced changes. Here, we are interested in the naturally varying strength of the stratospheric global circulation and how this impacts the composition of the stratosphere. Using observations and model simulations, we show that slowly changing (multi-decadal) natural variability in the Pacific Ocean is reflected in the stratospheric circulation. This link helps us to better understand structural changes in the stratospheric circulation arising due to human interferences. In turn, slow transport variability reconciles recent low levels of ozone in the middle tropical stratosphere, which otherwise are in disagreement with the expected ozone recovery. These results have implications for both reconciling theory and observed changes in the stratospheric circulation, as well as better understanding the rate of stratospheric ozone recovery.

Key Points:

- Low-frequency variability in the Brewer-Dobson circulation is coupled with low-frequency Pacific Ocean sea surface temperature variability
- Accounting for this allows the detection of an enhanced Brewer-Dobson circulation trend in model hindcasts of 7%–10% dec^{-1} over 1979–2010
- The low frequency variability also explains 50% of the observed trends in mid-stratospheric tropical ozone from 1990 to 2010

Supporting Information:

Supporting Information may be found in the online version of this article.

Correspondence to:

F. Iglesias-Suarez,
figlesua@gmail.com

Citation:

Iglesias-Suarez, F., Wild, O., Kinnison, D. E., Garcia, R. R., Marsh, D. R., Lamarque, J.-F., et al. (2021). Tropical stratospheric circulation and ozone coupled to Pacific multi-decadal variability. *Geophysical Research Letters*, *48*, e2020GL092162. https://doi.org/10.1029/2020GL092162

Received 16 DEC 2020
Accepted 19 MAY 2021

Author Contributions:

Conceptualization: Fernando Iglesias-Suarez, Paul J. Young
Formal analysis: Fernando Iglesias-Suarez
Methodology: Fernando Iglesias-Suarez, Paul J. Young
Resources: Douglas E. Kinnison, Rolando R. Garcia, Daniel R. Marsh, Jean-François Lamarque, Sean M. Davis
Writing – original draft: Fernando Iglesias-Suarez, Oliver Wild, Alfonso Saiz-Lopez, Paul J. Young

1. Introduction

The global mass circulation in the stratosphere, and stratosphere-troposphere exchange, is controlled by the Brewer-Dobson circulation (BDC), the global zonal-mean meridional circulation characterized by upwelling in the tropics along with poleward flow and downwelling at mid and high latitudes (Butchart, 2014). Multiple modeling studies have suggested an acceleration of the BDC since the mid twentieth century, associated with increasing atmospheric concentrations of greenhouse gases and rising sea surface temperatures (SSTs), as well as stratospheric ozone depletion (Oberländer-Hayn et al., 2015). This long-term trend is projected to continue this century (Butchart et al., 2010; Eichinger et al., 2019). However, there is also considerable variability in the strength of the BDC over shorter time scales (Aschmann et al., 2014),

Writing – review & editing: Oliver Wild, Douglas E. Kinnison, Rolando R. Garcia, Daniel R. Marsh, Jean-François Lamarque, Edmund M. Ryan, Sean M. Davis, Roland Eichinger, Alfonso Saiz-Lopez, Paul J. Young

which compromises our ability to detect anthropogenically forced changes in relatively short observationally derived data sets (Engel et al., 2009; Hegglin et al., 2014; Ray et al., 2014).

Inter-annual variability in the BDC is coupled to modes of natural variability, including El Niño/Southern Oscillation (ENSO) (Calvo et al., 2010; Marsh & Garcia, 2007), the quasi-biennial oscillation (QBO), and natural forcings (e.g., volcanic eruptions) (Abalos et al., 2015; Garfinkel et al., 2017). Indeed, sub-decadal SST variability in the tropical Pacific Ocean associated with ENSO has been linked to interannual changes in lower stratospheric tropical upwelling (Diallo et al., 2019), with a small (0.8%) but significant influence extending to the tropical middle stratosphere (Marsh & Garcia, 2007). On multi-decadal time scales, low frequency variability in the troposphere has been shown to impact the lower stratosphere and its circulation (Hu et al., 2018; Jadin et al., 2010), but the coupling to higher altitudes is less well understood, including any impacts on stratospheric composition.

The coupling of stratospheric variability to the Pacific Ocean is particularly noteworthy given that decadal SST variability in this region has been mooted as an important driver of the slowdown in global mean surface temperature trends at the start of the century (Kosaka & Xie, 2013), associated with changes in the trade winds (England et al., 2014) and deep ocean heat-uptake (Guemas et al., 2013). At the same time, despite falling concentrations of ozone depleting substances and the first signs of global stratospheric ozone recovery (Chipperfield et al., 2017), there have been decreases in tropical mid-stratospheric ozone since ~1991 (Nedoluha et al., 2015). Although the inflection point of ozone depletion in non-polar regions due to long-lived halogens occurred around year 1997 (WMO, 2007), in this equatorial region near 30 km (~10 hPa), ozone loss rates are most sensitive to reactive nitrogen (NO_y) abundance (Lary, 1997; Portmann et al., 2012), with ozone variability being determined by both NO_y source gas emissions (nitrous oxide, N_2O) and changes in atmospheric transport (Galytska et al., 2019).

In this study, we use measurements and chemistry-climate model simulations to explore the connection between Pacific Ocean low-frequency variability, the strength of the advective BDC, and the subsequent effect on tropical mid-stratosphere ozone levels. We demonstrate that accounting for multi-decadal SST variability, in the form of the Interdecadal Pacific Oscillation (IPO), can both reconcile long-term changes in the BDC in models and measurements, and account for recent trends in mid-stratospheric tropical ozone. Resulting changes in ozone levels are explained through impacts on tracer transport and nitrogen-catalyzed chemistry. This result is crucial to better understand dynamical and chemical processes in the stratosphere and to distinguish between natural and forced signals.

2. Data Sources: Chemistry-Climate Model Simulations and Observations

2.1. Chemistry-Climate Model Simulations

The Community Earth System Model, version 1 (CESM1) is a global climate model with active coupled land, ocean and sea ice components. The atmosphere component is the Whole Atmosphere Community Climate Model (WACCM), version 4, with an approximate horizontal resolution of 1.9° latitude by 2.5° longitude, and 66 vertical levels that extend to ~140 km (Marsh et al., 2013). The Model for Ozone and Related Chemical Tracers (MOZART) is the chemistry scheme (Kinnison et al., 2007), which includes full atmospheric chemistry from the troposphere to the lower thermosphere with gas-phase reactions, heterogeneous chemistry and photolysis (Eyring, Arblaster, et al., 2013; Eyring, Lamarque, et al., 2013).

The role of different forcings was explored using monthly mean output from the configuration of CESM1(WACCM) used in the Chemistry-Climate Model Initiative (CCMI) (Eyring, Arblaster, et al., 2013; Eyring, Lamarque, et al., 2013); this configuration couples the atmosphere and land components but is forced with observed SSTs, sea-ice concentrations, solar spectral irradiance, volcanic aerosols and near-equatorial winds constrained by observations of the QBO (Morgenstern et al., 2017; Tilmes et al., 2016). Monthly and seasonally varying boundary conditions were specified for radiatively active species, as well as long-lived halogen-containing species following the World Meteorological Organization's A1 halogen scenario (WMO, 2011). The version of CESM1(WACCM) used here includes MOZART version 4 (Emmons et al., 2010) and recent updates on photolysis, gas-phase and heterogeneous chemistry in the troposphere and the stratosphere (Lamarque et al., 2012; Tilmes et al., 2015).

To explore unforced variability in the stratosphere, we used monthly mean output from a pre-industrial control simulation (PI-CNTRL) of CESM1-WACCM. Our base case simulation (BASE) had all the boundary conditions evolving for the period 1960–2010 according to observations. In addition, four sensitivity simulations were performed to attribute recent changes in ozone: (a) nitrous oxide and long-lived halogen substances fixed at 1955 levels (Fixed N_2O-LL_{Hal}), (b) long-lived halogenated substances fixed at 1955 levels (Fixed LL_{Hal}), (c) background stratospheric aerosol (surface area densities) fixed at 1998–1999 averaged conditions (No Volcanoes; i.e., quiescent period without major volcanic eruptions as recommended by the CCMI activity; Eyring, Arblaster, et al., 2013; Eyring, Lamarque, et al., 2013), and (d) climatological SSTs and sea-ice concentrations averaged over 1960–2010 (i.e., a period with approximately equal positive-negative IPO phases) and with a cyclical QBO (i.e., a 28-month repeating cycle), namely Fixed SSTs. A cyclical QBO was imposed in the latter simulation to avoid any potential link between the Pacific Ocean's SSTs and the QBO at interannual (e.g., Schirber, 2015; and references therein) and multi-decadal time scales (Figures S1 and S2).

2.2. Ozone and Sea-Surface Temperature Observations, and the IPO Index Calculation

Stratospheric ozone trends were calculated using observations from the Stratospheric Water and OzOne Satellite Homogenized (SWOOSH) data set, version 2.6 (Davis et al., 2016) from 1984 to 2010. SWOOSH merges data from a range of satellites, which are homogenized and account for inter-satellite biases. The data are vertically resolved (31 levels from 316 to 1 hPa), zonal and monthly mean ozone mixing ratios with a horizontal resolution of 2.5°.

We use the Tripole Index (Henley et al., 2015) for the IPO. This is constructed as the residual of area-averaged, de-seasonalized SSTs across three rectangular regions: SSTs over 25°N-45°N, 140°E-145°W and 50°S-15°S, 150°E-160°W are subtracted from the mean of SSTs across 10°N-10°N, 170°E-90°W. Finally, a Chebyshev low-pass filter was applied, using a 13-year cutoff period and a filter order of six (i.e., local maximum in the variance that is coherent with the low-frequency portion of the IPO). SSTs to calculate the observed IPO index were taken from the NOAA Extended Reconstructed Sea Surface Temperature (ERSST) data set, version 5 (Huang et al., 2017). The ERSST reconstruction includes monthly data with horizontal resolution of 2° × 2° (latitude by longitude).

3. The Interdecadal Pacific Oscillation, Brewer-Dobson Circulation, and Tropical Mid-Stratospheric Ozone Link

We first use our pre-industrial control (PI-CNTRL) and recent past (BASE) simulations to demonstrate the dynamical and chemical drivers of multi-decadal tropical mid-stratosphere variability, in particular the relationship of the BDC and ozone with the IPO. Throughout, we diagnose the advective BDC strength from the Transformed Eulerian Mean vertical velocity, $\overline{w}^*$, in spherical and log pressure coordinates (Andrews et al., 1987).

Figure 1 shows the low-pass filtered annual mean time-series of standardized anomalies for the IPO index and the mid-stratosphere tropical (20°N-20°S and 5–10 hPa) average $\overline{w}^*$ for the PI-CNTRL (Figure 1a; 200 years of internally generated variability) and BASE (Figure 1b; 50 years of observed climate variability) simulations. The multi-decadal variability in Pacific Ocean SSTs associated with the IPO (red curves) is strongly correlated with changes in the BDC (orange curves) in this region for both the unforced (i.e., natural variability) PI-CNTRL ($r = 0.74$, $p < 0.01$) and forced (i.e., according to observations) BASE ($r = 0.79$, $p < 0.01$) simulations.

This variability in the BDC affects the stratospheric chemistry and composition, as demonstrated by a strong positive correlation and significant linear relationship between ozone (blue curves) and the strength of the BDC for both PI-CNTRL ($r = 0.95$, $p < 0.01$; slope 2.6% ± 0.1%/10 mm s^{-1}, ±2 standard error as a metric of the 95% confidence interval unless otherwise specified) and BASE ($r = 0.89$, $p < 0.01$; slope 4.0% ± 0.6%/10 mm s^{-1}) simulations, and therefore also between ozone and the IPO (Figures 1c and 1d; see Figure S3 for ozone evaluation). Although there are differences in the magnitude of the regression coefficient compared to observations (Figure S4), these simulations capture the fingerprint of the IPO in

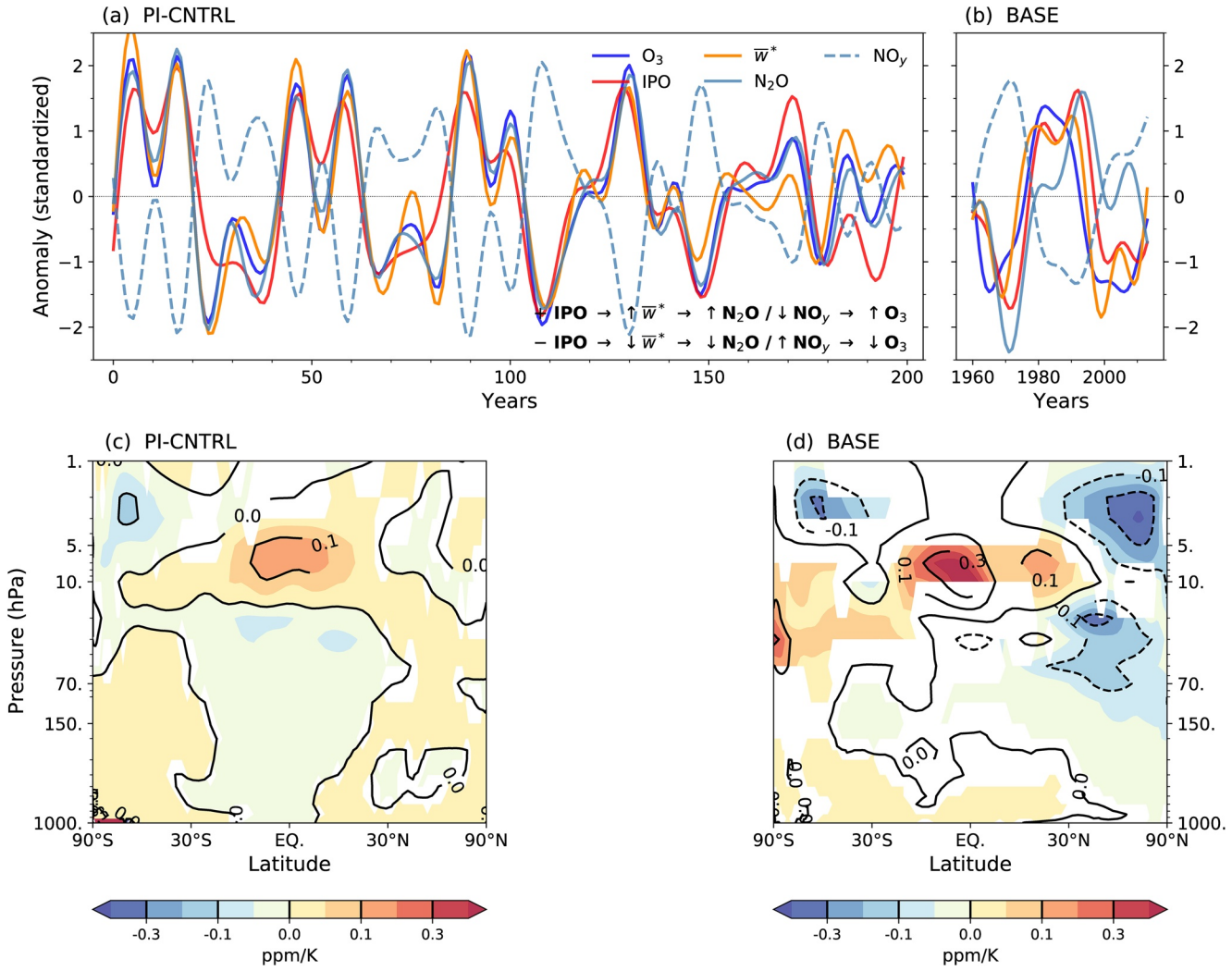

Figure 1. Simulated dynamical and chemical processes linking the Interdecadal Pacific Oscillation (IPO) with the tropical middle stratosphere. Low pass-filtered annual mean anomalies (standardized) of the IPO (solid red line), and the residual mean vertical velocity as a surrogate of the BDC ($\overline{w}^*$; solid orange line), N_2O (solid light-blue line), NO_y (dashed light-blue line) and ozone (O_3, solid blue line) averaged between 20°N-20°S and 5–10 hPa, for (a) the PI-CNTRL simulation (200 years with pre-industrial boundary conditions) and (b) the BASE simulation (1960–2010). The two lower panels show the zonal mean regression between the IPO and ozone for (c) the PI-CNTRL and (d) the BASE simulations. Shading indicates statistically significant regression between the IPO and ozone at the 5% level.

stratospheric ozone. While temperature changes in the tropical middle stratosphere modulate ozone loss (Haigh & Pyle, 1982; Rosenfield et al., 2002), catalytic NO_y chemistry is the most important ozone loss driver in this region (Lary, 1997), via reactions of NO with O_3 and NO_2 with O_2, resulting in the net conversion of O_3 and O into $2O_2$. The abundance of NO_y species is controlled by N_2O entering the stratosphere and by dynamics (Portmann et al., 2012). Due to the interaction of chemical and transport time scales, a relatively rapid circulation results in a reduced production of NO from the reaction of N_2O with $O(^1D)$, and vice versa (Olsen et al., 2001). This is clearly evident in our simulations, where decadal-scale variability in mid-stratosphere NO_y concentrations (dashed, light-blue curves) is strongly negatively correlated with the BDC for PI-CNTRL ($r = -0.91$, $p < 0.01$; slope $-5.9\% \pm 0.4\%$/10 mm s^{-1}; Figure 1a) and is also a clear feature in BASE ($r = -0.62$, $p < 0.01$; slope $-5.5\% \pm 1.9\%$/10 mm s^{-1}; Figure 1b). The above relationships are based on instantaneous values, as no time delays are found in the fully coupled long-term PI-CNTRL simulation. Time delays in the BASE simulation (not taken into account here) are more complex since it is a relatively short integration compared to the IPO variability which additionally includes varying forcings (e.g., volcanic eruptions and changes in N_2O emissions).

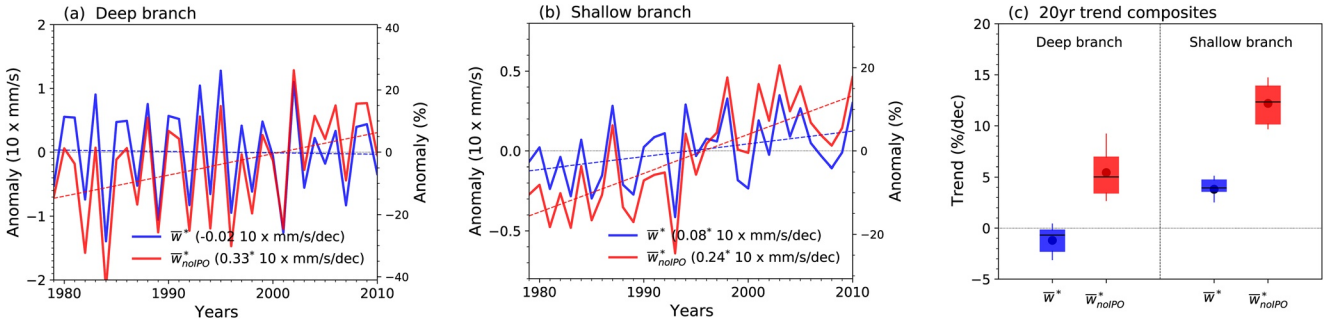

Figure 2. Modeled recent past trends in the Brewer-Dobson circulation from the BASE simulation, over 1979–2010. Annual mean anomalies of the residual mean vertical velocity with ($\overline{w}^*$; solid blue line) and without ($\overline{w}^*_{\mathrm{noIPO}}$, solid red line) the IPO, averaged over 20°N-20°S for the (a) deep (10 hPa; 0.49 mm s^{-1} climatological mean) and (b) shallow (70 hPa; 0.26 mm s^{-1} climatological mean) branches. Least squares linear trends are shown in brackets for $\overline{w}^*$ (dashed blue line) and $\overline{w}^*_{\mathrm{noIPO}}$ (dashed red line) from 1979 to 2010, approximately coinciding with previous observational and assimilated data studies (asterisks indicates statistically significant trends at the 5% level). (c) Composites of 20-year running trends for the shallow and deep BDC branches, for $\overline{w}^*$ (blue) and $\overline{w}^*_{\mathrm{noIPO}}$ (red). The box, whiskers, dot, and line indicate the interquartile range, 2.5th and 97.5th percentiles of the distribution, mean, and median respectively.

Overall, these simulations support a mechanism that couples dynamical (i.e., BDC) and chemical (i.e., ozone loss via NO_y chemistry) processes to explain this IPO-BDC-ozone link, which is in agreement with current process understanding (Galytska et al., 2019; Nedoluha et al., 2015; Plummer et al., 2010). A positive phase of the IPO (anomalously warm tropical SSTs) is associated with a relatively rapid BDC in the lower and middle stratosphere. In turn, this decreases the partitioning from inactive to reactive nitrogen species (N_2O to NO_y), which reduces ozone loss. The net result is a high ozone anomaly, whereas the opposite is true during a negative phase of the IPO. This low-frequency signal due to changes in SSTs in the middle stratosphere in CESM1(WACCM) may arise from longer and sustained conditions in the background climate state associated with the position of the subtropical tropospheric jets (Palmeiro et al., 2014) and decadal variability in the QBO (see Figure S1). The IPO signal in the tropical stratosphere is analogous to that of ENSO at shorter time scales (Diallo et al., 2019; Marsh & Garcia, 2007).

Although the Pacific Ocean's SSTs are a major source of decadal variability, other sources of internally generated variability may remain, such as the Atlantic Multi-decadal Oscillation and the Indo-Pacific heating (Lee et al., 2015; Wu et al., 2011), with significant impacts in global mean surface temperature variability (Nieves et al., 2015; Trenberth & Fasullo, 2013). Furthermore, while the IPO index is used here as a proxy for multi-decadal variability in the Pacific Ocean, we acknowledge that the IPO is not a single phenomenon but rather a combination of various physical processes dominated by ENSO-like decadal variability (Newman et al., 2016). The Pacific Decadal Oscillation (PDO) is a similar proxy, but not equivalent, being more influenced by the Aleutian Low (Mantua et al., 1997). Nevertheless, we find strong association between the low pass filtered IPO and PDO indexes from 1960 to 2010 ($r \approx 0.84$, $p < 0.01$) for both the ERSST database and the BASE simulation.

4. A Role for the IPO in Modulating Recent BDC Trends

We investigate next how the signal of the IPO impacts our understanding of recent stratospheric circulation trends. Figure 2 shows the trends in the annual mean BDC for the BASE simulation over 1979–2010. Focusing on this period allows us to explore the impact of the shift in the IPO from a positive to a negative phase, occurring between 1990 and 2000. Figures 2a and 2b present time series of the tropical average (20°N-20°S) upwelling, $\overline{w}^*$, as well as the upwelling in the absence of IPO-driven variability, $\overline{w}^*_{\mathrm{noIPO}}$, for the deep (10 hPa) and shallow (70 hPa) branches of the BDC, respectively. The $\overline{w}^*_{\mathrm{noIPO}}$ time-series removes the relationship between the IPO and BDC (Figure 1) and is calculated from

$$\overline{w}^*_{\mathrm{noIPO}} = \overline{w}^* - \frac{\partial \overline{w}^*}{\partial \mathrm{IPO}} \times \mathrm{IPO},$$

where the right-hand term describes the component of $\overline{w}^*$ linearly congruent with the low pass filtered annual mean anomalies of the IPO for the deep (slope 0.032 mm s^{-1} K^{-1}) and shallow (slope 0.018 mm s^{-1} K^{-1}) branches using the PI-CNTRL simulation (i.e., the IPO signal is unequivocally orthogonal to the long-term trend in the BASE simulation).

By accounting for the IPO-like variability in the BDC time-series, we can analyze the long-term residual signal, which may be linked to the increase in the greenhouse gas concentrations and ozone depletion in the last decades (Butchart et al., 2010). Over the 32-year period, $\overline{w}^*$ shows a significant positive decadal trend in the shallow branch (3.1% ± 2.8% dec^{-1}) but a non-significant trend in the deep branch (−0.4% ± 5.8% dec^{-1}). However, $\overline{w}^*_{\mathrm{noIPO}}$ shows steeper and statistically significant positive trends in both branches: 9.3% ± 3.1% dec^{-1} for the shallow branch and 6.8% ± 6.0% dec^{-1} for the deep branch. These regression-based changes in the BDC associated with the IPO are in agreement with the Fixed SSTs sensitivity simulation (Figure S2), though in the latter the signal is somewhat weaker.

Figure 2c shows the sensitivity of the BDC linear trend estimates to different periods and end points, showing the trends calculated for successive 20-year periods (1979–1998, 1980–1999, etc.) to illustrate the robustness of secular changes in the shallow and deep branches over 1979–2010. The 20-year running trend composites (12 individual trends) of $\overline{w}^*$ show a mean positive trend in the shallow branch significant at the 5% level (3.8% dec^{-1}), and again, an insignificant negative trend in the deep branch (−1.2% dec^{-1}), consistent with the above results. For the 20-year trends in $\overline{w}^*_{\mathrm{noIPO}}$, both the shallow (12.2% dec^{-1}) and deep (5.4% dec^{-1}) branches show a mean positive and significant trend regardless the chosen period: between approximately 10.2%–13.9% dec^{-1} for the shallow branch and 3.4%–6.9% dec^{-1} for the deep branch, using the interquartile ranges. Note that increasing the length over which the successive linear trends are calculated greatly reduces the variance (not shown), which also means that the BDC trends for relatively short periods (including current observational data sets) are highly sensitive to the particular period chosen.

Our analysis demonstrates that accounting for unforced climate variability can help in bridging the gap between previous estimates of BDC trends, particularly for the deep branch, and their consistency with theory and simulation-based calculations. Despite the general agreement of the acceleration in the shallow branch, the overall picture of trends over the last three or so decades from observationally based (Engel et al., 2009; Hegglin et al., 2014; Ray et al., 2014; Young et al., 2012) and reanalysis-based (Abalos et al., 2015; Bönisch et al., 2011; Diallo et al., 2012; Monge-Sanz et al., 2013; Seviour et al., 2012; Yuan et al., 2015) studies is somewhat inconclusive for the deep branch, reporting no trends, negative trends or differing trends. We acknowledge that the majority of the studies above are tracer-based and hence include mixing, which can influence BDC diagnostics (Dietmüller et al., 2018; Eichinger et al., 2019). Nevertheless, in our BASE simulation, which captures real-world interannual variability, accounting for the influence of the IPO unmasks a robust positive trend in the deep branch of the advective BDC not apparent in the "raw" model output. This trend, also positive but weaker compared to the shallow branch, is more consistent with the plethora of long-term climate model studies that report a strengthening of the BDC under different emission scenarios (Butchart, 2014; Dietmüller et al., 2018).

5. IPO, BDC, and Ozone Coupling in the Recent Past

Having demonstrated the importance of IPO-like variability for unforced variability in the BDC, and proposed a mechanism to couple this IPO-like variability in the BDC with mid-stratospheric ozone, we finally turn to consider their roles in recent ozone trends (Nedoluha et al., 2015). Figure 3a presents time-series of simulated mid-stratospheric tropical (20°N-20°S) and annual average ozone anomalies, smoothed with a 10-years running mean, between 1960 and 2010 for several simulations. The BASE simulation (blue curve) is in good agreement with observationally based estimates (black curve) for both the simulated 10-years running mean ozone trends for the 1990–2000 period (Table 1) and for the annual mean ozone over the 1984–2010 period ($r = 0.72$, $p < 0.01$; Figure S3). The latter period encompasses a shift from a positive to a negative IPO phase, as indicated by the low-pass filtered IPO index in Figure 3b.

From 2000 on, simulated ozone levels in this region are persistently low, which is consistent with the proposed mechanism and the negative phase of the IPO (Figure 3a). Internally generated SST variability, particularly in the tropics (i.e., IPO regression pattern; Figure S5a), drives changes in the strato-

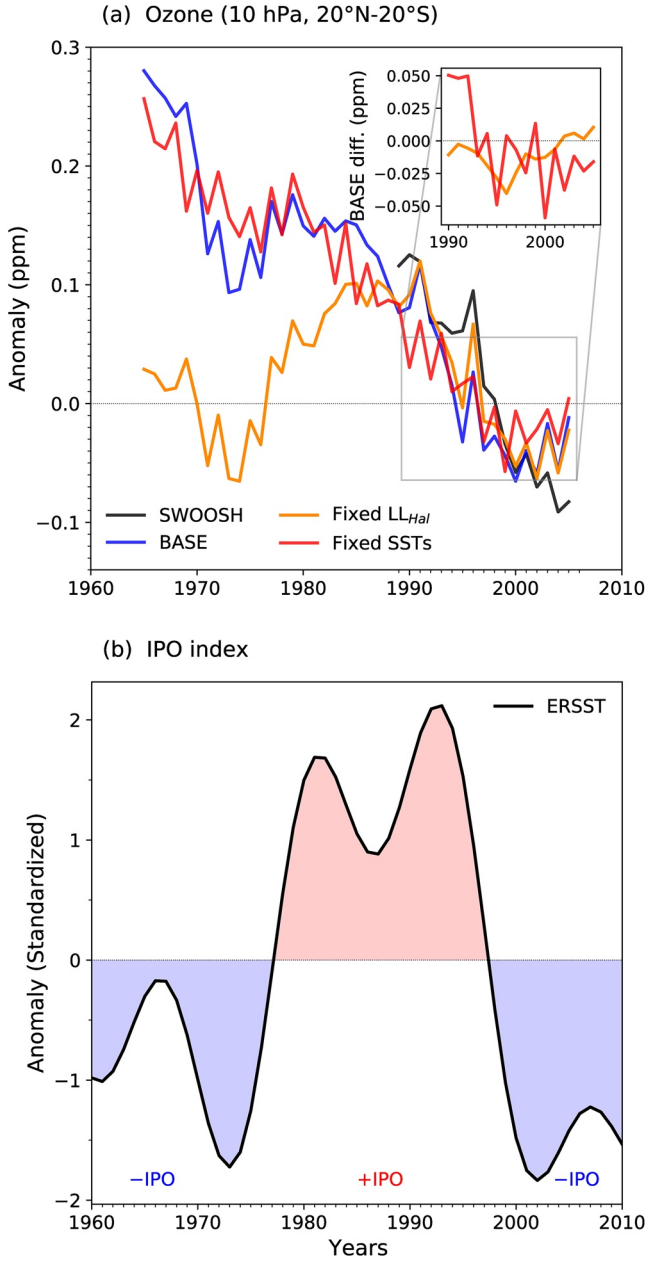

Figure 3. Changes in mid-stratospheric tropical ozone and the IPO. (a) 10-Year running annual mean of tropical average (20°N-20°S) ozone at 10 hPa, expressed as an anomaly relative to 1984–2010, for the Stratospheric Water and Ozone Satellite Homogenized (SWOOSH version 2.6) data base (solid black line) and the BASE simulation (as per the "real world"; blue line). Also, shown are ozone time-series, but with fixed anthropogenic long-lived halogens (Fixed LL_{Hal}; orange line) and with a seasonally varying climatological mean SSTs (Fixed SSTs; red line). The inset shows the difference between the BASE simulation and the Fixed LL_{Hal} and Fixed SSTs sensitivity cases. (b) A standardized, low-pass filtered annual mean anomaly IPO index relative to 1960–2010, calculated from the ERSST sea-surface temperature data set.

spheric circulation. During the first decade of the 21st century, anomalously cold tropical SSTs (Figure S5b) compared to the 1980–1990 period are consistent with both the negative phase of the IPO and a relatively weaker BDC. As argued above, the associated reduced vertical transport in the middle tropical stratosphere is, in turn, linked to lower ozone levels via enhanced NO_y-catalyzed ozone loss (i.e., greater N_2O photo-oxidation resulting from longer transport time scales; Figure S6d). These results are in agreement with observed increases in tropical total column ozone in the recent past, associated with long-term variability in ENSO and a relatively weaker tropical upwelling (Coldewey-Egbers et al., 2014).

However, a number of drivers could also be playing a role in these recent (since ~1990) changes in mid-stratospheric tropical ozone, particularly those that involve changes in anthropogenic long-lived halogen (LL_{Hal}) and N_2O concentrations, as well as stratospheric volcanic aerosols (Garfinkel et al., 2017; Portmann et al., 2012; WMO, 2018). Table 1 and Figure 3 show an assessment of the relative importance of these drivers, through our series of sensitivity simulations where individual drivers are held fixed (see Section 2.1). Note that, to enhance readability of the plot, not every simulation is shown in Figure 3, but the contribution of each driver is listed in Table 1. Assuming that these drivers affect ozone in a linear manner, N_2O and LL_{Hal} together account for around a fifth of the simulated 1990–2000 trend (Fixed N_2O-LL_{Hal}); major volcanic eruptions, El Chichón (year 1982) and Mt Pinatubo (year 1991), explain an additional quarter of the trend (No Volcanoes); and the natural variability in SSTs accounts for about half of the trend (Fixed SSTs; see inset in Figure 3a). The response of ozone in the middle tropical stratosphere to slowly varying SSTs is clearly shown by the Fixed LL_{Hal} sensitivity simulation (orange curve in Figure 3a), which evolves like the IPO index (Figure 3b) throughout 1960–2010. While the overall ozone destruction by ozone depleting substances is captured by the Fixed SSTs simulation, it does not capture the BASE simulation ozone variability since 1990, whereas this is evident in Fixed LL_{Hal}. In this region, removing the warming trend in SSTs in the Fixed SSTs simulation has a negligible influence on ozone concentrations (not shown). Overall, these results indicate that recent negative trends in ozone (since about 1990) in the tropical middle stratosphere are not primarily the result of anthropogenic emissions (N_2O and LL_{Hal}) but instead are dominated by low frequency variability in the BDC tied to the Pacific Ocean's SSTs.

6. Conclusions

Current climate models show a long-term acceleration of the stratospheric Brewer-Dobson circulation due to increasing greenhouse gas concentrations and stratospheric ozone depletion (Butchart, 2014). However, in the middle and upper stratosphere, the observational (Engel et al., 2009) and reanalysis (Abalos et al., 2015; Bönisch et al., 2011; Diallo et al., 2012) evidence for this acceleration has been somewhat equivocal, due to relatively large uncertainties in short periods (<25 years) associated with natural variability (Garfinkel et al., 2017). In addition, in spite of first signs of global stratospheric ozone recovery (Chipperfield et al., 2017), changes in atmospheric transport have

Table 1
Trends in Mid-Stratospheric (10 hPa) Tropical Average (20°N-20°S) Ozone Between 1990 and 2000 for Observations and the BASE Simulation of the 10-Year Running Means, Including Individual Contributions of Key Drivers

		Contribution[a] of individual drivers			
Observations[b]	BASE[c]	Fixed N_2O-LL_{Hal}[d]	Fixed LL_{Hal}[d]	No Volcanoes[d]	Fixed SSTs[d]
-0.16 ± 0.07 ppm dec^{-1}	-0.17 ± 0.07 ppm dec^{-1}	22.1%	6.5%	25.8%	49.1%[e]

Note. The least squared linear decadal trend is given along with the (±2) standard error accounting for 1-lag autocorrelation of the regression residuals.

[a]Contributions are for the difference between the individual sensitivity simulations and the BASE simulation expressed in percentage. [b]From the Stratospheric Water and Ozone Satellite Homogenized (version 2.6) database (Davis et al., 2016). [c]The base simulation using CESM1-WACCM driven by all the observed boundary conditions. [d]Attribution of mid-stratospheric tropical ozone trends to Fixed N_2O-LL_{Hal}, Fixed LL_{Hal}, No Volcanoes, and Fixed SSTs respectively, derived from a series of CESM1-WACCM sensitivity simulations. See text for details. [e]Statistically significant differences in the trend compared to the BASE simulation (at the 5% level).

been suggested as the driver of recent declines in tropical mid-stratospheric ozone (Galytska et al., 2019; Nedoluha et al., 2015).

In the present study, we have used observations and the high-top, chemistry-climate model CESM1-WACCM, to explore the role of multi-decadal climate variability, associated with Pacific Ocean SSTs (as characterized by the Interdecadal Pacific Oscillation, IPO), in driving the circulation in the stratosphere and its composition. We show that after accounting for the IPO-like variability in the BDC, the simulated BDC trend is steeper and statistically significant at about 7%–10% over the 1979–2010 period for both the shallow and deep branches; hence, we argue that the IPO may well have masked, to some extent, the BDC acceleration during the observational record, particularly in the deep branch. Exploring the IPO-like variability in the BDC in other climate models would give us more insight into how the multi-decadal time scale circulation in the stratosphere is coupled to the troposphere. Furthermore, we find that sea surface temperatures explain approximately 50% of the simulated decadal variability in tropical mid-stratospheric ozone through dynamical (BDC) and chemical (nitrogen-catalyzed ozone loss) processes. We acknowledge that the IPO signal is not wholly isolated in our analysis and that the role of other aspects of internal variability, such as the Atlantic Multi-decadal Oscillation, remains to be explored, which may influence stratospheric dynamics and composition.

To sum up, this study demonstrates how internal climate variability on multi-decadal time scales can influence transport and composition in the stratosphere. It also highlights the need for a good representation of dynamical and chemical processes in climate models if they are to be used to distinguish between forced and unforced signals, including detecting ozone layer recovery.

Conflict of Interest

The authors declare no conflicts of interest relevant to this study.

Data Availability Statement

The observational data sets, SWOOSH version 2.6 (https://www.esrl.noaa.gov/csl/groups/csl8/swoosh/) and ERSST version 5 (https://www.ncdc.noaa.gov/data-access/marineocean-data/extended-reconstructed-sea-surface-temperature-ersst-v5), are publicly available. The CMIP5 data are available through the Earth System Grid Federation (https://esgf-node.llnl.gov/search/cmip5/). The CCMI data of the CESM1-WACCM model are available through the NCAR Climate Data Gateway (https://www.earthsystemgrid.org). Data of our sensitivity simulations using CESM1-WACCM are available at Zenodo (https://doi.org/10.5281/zenodo.4282423). The software code for the CESM1 model is available from http://www.cesm.ucar.edu/models. Python open-source software used in this analysis is publicly available (https://www.python.org).

Acknowledgments
The authors thank Anne K. Smith, Michael J. Mills, and Robert W. Portman for a helpful discussion on stratospheric variability and chemical processes. This work was supported by the UK Natural Environment Research Council (projects NE/L501736/1 and NE/R004927/1), Engineering and Physical Sciences Research Council (project EP/R01860X/1), Helmholtz Association grant VH-NG-1014 (Helmholtz-Hochschulachwuchsforscher gruppe MACClim), and Czech Science Foundation (GACR) grants (16-01562J and 18-01625S). CESM1-WACCM, which is supported by the NSF and the Office of Science of the U.S. Department of Energy. Computing resources were provided by NCAR's Climate Simulation Laboratory, sponsored by the NSF and other agencies. This research was enabled by the computational and storage resources of NCAR's Computational and Information Systems Laboratory (CISL). Open access funding enabled and organized by Projekt DEAL.

References

Abalos, M., Legras, B., Ploeger, F., & Randel, W. J. (2015). Evaluating the advective Brewer-Dobson circulation in three reanalyzes for the period 1979–2012. *Journal of Geophysical Research: Atmospheres*, *120*(15), 7534–7554. https://doi.org/10.1002/2015JD023182

Andrews, D. G., Taylor, F. W., & McIntyre, M. E. (1987). The influence of atmospheric waves on the general circulation of the middle atmosphere [and Discussion]. *Philosophical Transactions of the Royal Society A: Mathematical, Physical & Engineering Sciences*, *323*(1575), 693–705. https://doi.org/10.1098/rsta.1987.0115

Aschmann, J., Burrows, J. P., Gebhardt, C., Rozanov, A., Hommel, R., Weber, M., & Thompson, A. M. (2014). On the hiatus in the acceleration of tropical upwelling since the beginning of the 21st century. *Atmospheric Chemistry and Physics*, *14*(23), 12803–12814. https://doi.org/10.5194/acp-14-12803-2014

Bönisch, H., Engel, A., Birner, T., Hoor, P., Tarasick, D. W., & Ray, E. A. (2011). On the structural changes in the Brewer-Dobson circulation after 2000. *Atmospheric Chemistry and Physics*, *11*(8), 3937–3948. https://doi.org/10.5194/acp-11-3937-2011

Butchart, N. (2014). The Brewer-Dobson circulation. *Reviews of Geophysics*, *52*, 157–184. https://doi.org/10.1002/2013RG000448

Butchart, N., Cionni, I., Eyring, V., Shepherd, T. G., Waugh, D. W., Akiyoshi, H., et al. (2010). Chemistry–climate model simulations of twenty-first century stratospheric climate and circulation changes. *Journal of Climate*, *23*(20), 5349–5374. https://doi.org/10.1175/2010JCLI3404.1

Calvo, N., Garcia, R. R., Randel, W. J., & Marsh, D. R. (2010). Dynamical mechanism for the increase in tropical upwelling in the lowermost tropical stratosphere during warm ENSO events. *Journal of the Atmospheric Sciences*, *67*(7), 2331–2340. https://doi.org/10.1175/2010JAS3433.1

Chipperfield, M. P., Bekki, S., Dhomse, S., Harris, N. R. P., Hassler, B., Hossaini, R., et al. (2017). Detecting recovery of the stratospheric ozone layer. *Nature*, *549*(7671), 211–218. https://doi.org/10.1038/nature23681

Coldewey-Egbers, M., Loyola, R. D. G., Braesicke, P., Dameris, M., Roozendael, M., Lerot, C., & Zimmer, W. (2014). A new health check of the ozone layer at global and regional scales. *Geophysical Research Letters*, *41*(12), 4363–4372. https://doi.org/10.1002/2014GL060212

Davis, S. M., Rosenlof, K. H., Hassler, B., Hurst, D. F., Read, W. G., Vömel, H., et al. (2016). The stratospheric water and ozone satellite homogenized (SWOOSH) database: A long-term database for climate studies. *Earth System Science Data*, *8*(2), 461–490. https://doi.org/10.5194/essd-8-461-2016

Diallo, M., Konopka, P., Santee, M. L., Müller, R., Tao, M., Walker, K. A., et al. (2019). Structural changes in the shallow and transition branch of the Brewer–Dobson circulation induced by El Niño. *Atmospheric Chemistry and Physics*, *19*(1), 425–446. https://doi.org/10.5194/acp-19-425-2019

Diallo, M., Legras, B., & Chédin, A. (2012). Age of stratospheric air in the ERA-Interim. *Atmospheric Chemistry and Physics*, *12*(24), 12133–12154. https://doi.org/10.5194/acp-12-12133-2012

Dietmüller, S., Eichinger, R., Garny, H., Birner, T., Boenisch, H., Pitari, G., et al. (2018). Quantifying the effect of mixing on the mean age of air in CCMVal-2 and CCMI-1 models. *Atmospheric Chemistry and Physics*, *18*(9), 6699–6720. https://doi.org/10.5194/acp-18-6699-2018

Eichinger, R., Dietmüller, S., Garny, H., Šácha, P., Birner, T., Bönisch, H., et al. (2019). The influence of mixing on the stratospheric age of air changes in the 21st century. *Atmospheric Chemistry and Physics*, *19*(2), 921–940. https://doi.org/10.5194/acp-19-921-2019

Emmons, L. K., Walters, S., Hess, P. G., Lamarque, J.-F., Pfister, G. G., Fillmore, D., et al. (2010). Description and evaluation of the Model for Ozone and Related chemical Tracers, version 4 (MOZART-4). *Geoscientific Model Development*, *3*(1), 43–67. https://doi.org/10.5194/gmd-3-43-2010

Engel, A., Möbius, T., Bönisch, H., Schmidt, U., Heinz, R., Levin, I., et al. (2009). Age of stratospheric air unchanged within uncertainties over the past 30 years. *Nature Geoscience*, *2*(1), 28–31. https://doi.org/10.1038/ngeo388

England, M. H., McGregor, S., Spence, P., Meehl, G. A, Timmermann, A., Cai, W., et al. (2014). Recent intensification of wind-driven circulation in the Pacific and the ongoing warming hiatus. *Nature Climate Change*, *4*(3), 222–227. https://doi.org/10.1038/NCLIMATE2106

Eyring, V., Arblaster, J. M., Cionni, I., Sedláček, J., Perlwitz, J., Young, P. J., et al. (2013). Long-term ozone changes and associated climate impacts in CMIP5 simulations. *Journal of Geophysical Research: Atmospheres*, *118*(10), 5029–5060. https://doi.org/10.1002/jgrd.50316

Eyring, V., Lamarque, J.-F., Hess, P., Arfeuille, F., Bowman, K., Chipperfield, M. P., et al. (2013). Overview of IGAC/SPARC chemistry-climate model initiative (CCMI) community simulations in support of upcoming ozone and climate assessments. *SPARC Newsletter*. *40*, p. 48–66.

Galytska, E., Rozanov, A., Chipperfield, M. P., Dhomse, S. S., Weber, M., Arosio, C., et al. (2019). Dynamically controlled ozone decline in the tropical mid-stratosphere observed by SCIAMACHY. *Atmospheric Chemistry and Physics*, *19*(2), 767–783. https://doi.org/10.5194/acp-19-767-2019

Garfinkel, C. I., Aquila, V., Waugh, D. W., & Oman, L. D. (2017). Time-varying changes in the simulated structure of the Brewer–Dobson circulation. *Atmospheric Chemistry and Physics*, *17*(2), 1313–1327. https://doi.org/10.5194/acp-17-1313-2017

Guemas, V., Doblas-Reyes, F. J., Andreu-Burillo, I., & Asif, M. (2013). Retrospective prediction of the global warming slowdown in the past decade. *Nature Climate Change*, *3*(4), 1–653. https://doi.org/10.1038/nclimate1863

Haigh, J. D., & Pyle, J. A. (1982). Ozone perturbation experiments in a two-dimensional circulation model. *Quarterly Journal of the Royal Meteorological Society*, *108*(457), 551–574. https://doi.org/10.1002/qj.49710845705

Hegglin, M. I., Plummer, D. A., Shepherd, T. G., Scinocca, J. F., Anderson, J., Froidevaux, L., et al. (2014). Vertical structure of stratospheric water vapor trends derived from merged satellite data. *Nature Geoscience*, *7*(10), 768–776. https://doi.org/10.1038/ngeo2236

Henley, B. J., Gergis, J., Karoly, D. J., Power, S., Kennedy, J., & Folland, C. K. (2015). A tripole index for the interdecadal Pacific oscillation. *Climate Dynamics*, *45*(11–12), 3077–3090. https://doi.org/10.1007/s00382-015-2525-1

Hu, D., Guan, Z., Hu, D., & Guan, Z. (2018). Decadal relationship between the stratospheric Arctic vortex and pacific decadal oscillation. *Journal of Climate*, *31*(9), 3371–3386. https://doi.org/10.1175/JCLI-D-17-0266.1

Huang, B., Thorne, P. W., Banzon, V. F., Boyer, T., Chepurin, G., Lawrimore, J. H., et al. (2017). Extended reconstructed sea surface temperature, version 5 (ERSSTv5): Upgrades, validations, and intercomparisons. *Journal of Climate*, *30*(20), 8179–8205. https://doi.org/10.1175/JCLI-D-16-0836.1

Jadin, E. A., Wei, K., Zyulyaeva, Y. A., Chen, W., & Wang, L. (2010). Stratospheric wave activity and the Pacific decadal oscillation. *Journal of Atmospheric and Solar-Terrestrial Physics*, *72*(16), 1163–1170. https://doi.org/10.1016/j.jastp.2010.07.009

Kinnison, D. E., Brasseur, G. P., Walters, S., Garcia, R. R., Marsh, D. R., Sassi, F., et al. (2007). Sensitivity of chemical tracers to meteorological parameters in the MOZART-3 chemical transport model. *Journal of Geophysical Research*, *112*(D20), D20302. https://doi.org/10.1029/2006JD007879

Kosaka, Y., & Xie, S.-P. (2013). Recent global-warming hiatus tied to equatorial Pacific surface cooling. *Nature*, *501*(7467), 403–407. https://doi.org/10.1038/nature12534

Lamarque, J. F., Emmons, L. K., Hess, P. G., Kinnison, D. E., Tilmes, S., Vitt, F., et al. (2012). CAM-chem: Description and evaluation of interactive atmospheric chemistry in the Community Earth System Model. *Geoscientific Model Development*, *5*(2), 369–411. https://doi.org/10.5194/gmd-5-369-2012

Lary, D. J. (1997). Catalytic destruction of stratospheric ozone. *Journal of Geophysical Research: Atmospheres*, *102*(D17), 21515–21526. https://doi.org/10.1029/97JD00912

Lee, S.-K., Park, W., Baringer, M. O., Gordon, A. L., Huber, B., & Liu, Y. (2015). Pacific origin of the abrupt increase in Indian Ocean heat content during the warming hiatus. *Nature Geoscience*, *8*(6), 445–449. https://doi.org/10.1038/ngeo2438

Mantua, N. J., Hare, S. R., Zhang, Y., Wallace, J. M., & Francis, R. C. (1997). A Pacific interdecadal climate oscillation with impacts on salmon production. *Bulletin of the American Meteorological Society*, *78*(6), 1069–1079. https://doi.org/10.1175/1520-0477(1997)078<1069:APICOW>2.0.CO;2

Marsh, D. R., & Garcia, R. R. (2007). Attribution of decadal variability in lower-stratospheric tropical ozone. *Geophysical Research Letters*, *34*(21), L21807. https://doi.org/10.1029/2007GL030935

Marsh, D. R., Mills, M. J., Kinnison, D. E., Lamarque, J. F., Calvo, N., & Polvani, L. M. (2013). Climate change from 1850 to 2005 simulated in CESM1(WACCM). *Journal of Climate*, *26*(19), 7372–7391. https://doi.org/10.1175/JCLI-D-12-00558.1

Monge-Sanz, B. M., Chipperfield, M. P., Dee, D. P., Simmonsc, A. J., & Uppalac, S. M. (2013). Improvements in the stratospheric transport achieved by a chemistry transport model with ECMWF (re)analyses: Identifying effects and remaining challenges. *Quarterly Journal of the Royal Meteorological Society*, *139*(672), 654–673. https://doi.org/10.1002/qj.1996

Morgenstern, O., Hegglin, M. I., Rozanov, E., O'Connor, F. M., Abraham, N. L., Akiyoshi, H., et al. (2017). Review of the global models used within phase 1 of the Chemistry–Climate Model Initiative (CCMI). *Geoscientific Model Development*, *10*(2), 639–671. https://doi.org/10.5194/gmd-10-639-2017

Nedoluha, G. E., Siskind, D. E., Lambert, A., & Boone, C. (2015). The decrease in mid-stratospheric tropical ozone since 1991. *Atmospheric Chemistry and Physics*, *15*(8), 4215–4224. https://doi.org/10.5194/acp-15-4215-2015

Newman, M., Alexander, M. A., Ault, T. R., Cobb, K. M., Deser, C., Di Lorenzo, E., et al. (2016). The Pacific decadal oscillation, revisited. *Journal of Climate*, *29*(12), 4399–4427. https://doi.org/10.1175/JCLI-D-15-0508.1

Nieves, V., Willis, J. K., & Patzert, W. C. (2015). Recent hiatus caused by decadal shift in Indo-Pacific heating. *Science*, *349*(6247), 532–535. https://doi.org/10.1126/science.aaa4521

Oberländer-Hayn, S., Meul, S., Langematz, U., Abalichin, J., & Haenel, F. (2015). A chemistry-climate model study of past changes in the Brewer-Dobson circulation. *Journal of Geophysical Research: Atmospheres*, *120*(14), 6742–6757. https://doi.org/10.1002/2014JD022843

Olsen, S. C., McLinden, C. A., & Prather, M. J. (2001). Stratospheric N_2O-NO_y system: Testing uncertainties in a three-dimensional framework. *Journal of Geophysical Research: Atmospheres*, *106*(D22), 28771–28784. https://doi.org/10.1029/2001JD000559

Palmeiro, F. M., Calvo, N., & Garcia, R. R. (2014). Future changes in the Brewer–Dobson circulation under different greenhouse gas concentrations in WACCM4. *Journal of the Atmospheric Sciences*, *71*(8), 2962–2975. https://doi.org/10.1175/JAS-D-13-0289.1

Plummer, D. A., Scinocca, J. F., Shepherd, T. G., Reader, M. C., & Jonsson, A. I. (2010). Quantifying the contributions to stratospheric ozone changes from ozone depleting substances and greenhouse gases. *Atmospheric Chemistry and Physics*, *10*(18), 8803–8820. https://doi.org/10.5194/acp-10-8803-2010

Portmann, R. W., Daniel, J. S., & Ravishankara, A. R. (2012). Stratospheric ozone depletion due to nitrous oxide: Influences of other gases. *Philosophical Transactions of the Royal Society B: Biological Sciences*, *367*(1593), 1256–1264. https://doi.org/10.1098/rstb.2011.0377

Ray, E. A., Moore, F. L., Rosenlof, K. H., Davis, S. M., Sweeney, C., Tans, P., et al. (2014). Improving stratospheric transport trend analysis based on SF6 and CO_2 measurements. *Journal of Geophysical Research: Atmospheres*, *119*(24), 110–114. https://doi.org/10.1002/2014JD021802

Rosenfield, J. E., Douglass, A. R., & Considine, D. B. (2002). The impact of increasing carbon dioxide on ozone recovery. *Journal of Geophysical Research: Atmospheres*, *107*(D6), ACH 7-1–ACH 7-9. https://doi.org/10.1029/2001JD000824

Schirber, S. (2015). Influence of ENSO on the QBO: Results from an ensemble of idealized simulations. *Journal of Geophysical Research: Atmospheres*, *120*(3), 1109–1122. https://doi.org/10.1002/2014JD022460

Seviour, W. J. M., Butchart, N., & Hardiman, S. C. (2012). The Brewer-Dobson circulation inferred from ERA-Interim. *Quarterly Journal of the Royal Meteorological Society*, *138*(665), 878–888. https://doi.org/10.1002/qj.966

Tilmes, S., Lamarque, J.-F., Emmons, L. K., Kinnison, D. E., Ma, P.-L., Liu, X., et al. (2015). Description and evaluation of tropospheric chemistry and aerosols in the Community Earth System Model (CESM1.2). *Geoscientific Model Development*, *8*(5), 1395–1426. https://doi.org/10.5194/gmd-8-1395-2015

Tilmes, S., Lamarque, J. F., Emmons, L. K., Kinnison, D. E., Marsh, D., Garcia, R. R., et al. (2016). Representation of the community earth system model (CESM1) CAM4-chem within the chemistry-climate model initiative (CCMI). *Geoscientific Model Development*, *9*(5), 1853–1890. https://doi.org/10.5194/gmd-9-1853-2016

Trenberth, K. E., & Fasullo, J. T. (2013). An apparent hiatus in global warming? *Earth's Future*, *1*(1), 19–32. https://doi.org/10.1002/2013EF000165.Received

WMO (2007). Scientific assessment of ozone depletion: 2006. Global Ozone Research and Monitoring Project (Vol. 50). World Meteorological Organization.

WMO (2011). Scientific assessment of ozone depletion: 2010. Global Ozone Research and Monitoring Project-Report (Vol. 52). Geneva, Switzerland: World Meteorological Organization.

WMO (2018). Scientific assessment of ozone depletion: 2018. Global Ozone Research and Monitoring Project-Report (Vol. 58). Geneva, Switzerland: World Meteorological Organization.

Wu, S., Liu, Z., Zhang, R., & Delworth, T. L. (2011). On the observed relationship between the Pacific decadal oscillation and the Atlantic multi-decadal oscillation. *Journal of Oceanography*, *67*(1), 27–35. https://doi.org/10.1007/s10872-011-0003-x

Young, P. J., Rosenlof, K. H., Solomon, S., Sherwood, S. C., Fu, Q., & Lamarque, J.-F. (2012). Changes in stratospheric temperatures and their implications for changes in the Brewer-Dobson circulation, 1979–2005. *Journal of Climate*, *25*(5), 1759–1772. https://doi.org/10.1175/2011jcli4048.1

Yuan, N., Ding, M., Huang, Y., Fu, Z., Xoplaki, E., & Luterbacher, J. (2015). On the long-term climate memory in the surface air temperature records over Antarctica: A non-negligible factor for trend evaluation. *Journal of Climate*, *28*, 5922–5934. https://doi.org/10.1175/JCLI-D-14-00733.1